

Static Antiwindup Design for Nonlinear Parameter Varying Systems With Application to DC Motor Speed Control Under Nonlinearities and Load Variations

Najam us Saqib, Muhammad Rehan, Naeem Iqbal, and Keum-Shik Hong, *Senior Member, IEEE*

Abstract—In this brief, a novel scheme to design an antiwindup gain by ensuring local stability for nonlinear parameter varying systems having an input saturation is derived. Antiwindup compensator (AWC) design is provided for a dynamic output feedback controller that meets the desired closed-loop stability and performance specifications in the absence of the input saturation. A linear matrix inequality-based condition by application of Lyapunov theory, a local sector condition, an upper bound on the nonlinearity, and parametric bounds is formulated for the AWC design to ensure asymptotic and \mathcal{L}_2 stability. In contrast to the conventional approaches for nonlinear systems, the proposed AWC approach accounts for parametric variations, considers computationally simple static antiwindup, is straightforward for implementation, is useful for the existing control system, and can reduce the design conservatism. The proposed AWC design approach is tested for a practical scenario on the dc servo system control under armature nonlinearity, load variations, and control input saturation. Both simulation and experimental results are provided.

Index Terms—Antiwindup compensator (AWC), load variations, local stability, motor speed control, nonlinear parameter varying (NPV) systems.

I. INTRODUCTION

THE ACTUATOR of a linear or a nonlinear system is always subjected to the lower and the upper magnitude limits, causing saturation of a control signal. Usually, the actuator saturation is ignored to simplify the design of a feedback controller, which induces undesirable effects like performance degradation, overshoot, undershoot, lag, and instability of a closed-loop system response as a consequence of the windup phenomenon [1]–[4]. In order to cope with the problems of the input saturation, an antiwindup compensator (AWC) is employed, in addition to the existing feedback controller, to ensure global or local stability of the closed-loop system.

Manuscript received November 16, 2016; revised February 3, 2017; accepted March 28, 2017. Date of publication April 25, 2017; date of current version April 11, 2018. Manuscript received in final form March 31, 2017. Recommended by Associate Editor E. Usai. This work was supported by the Higher Education Commission of Pakistan through Indigenous Ph.D. Scholarship Phase II Batch II and the National Research Foundation of Korea under the auspices of the Ministry of Science, ICT, and Future Planning, South Korea, under Grant NRF-2014-R1A2A1A10049727. (Corresponding author: Muhammad Rehan.)

N. us Saqib, M. Rehan, and N. Iqbal are with the Department of Electrical Engineering, Pakistan Institute of Engineering and Applied Sciences, Islamabad 45650, Pakistan (e-mail: nsaqib83@gmail.com; rehanqau@gmail.com; naeem@pieas.edu.pk).

K.-S. Hong is with the Department of Cogno-Mechatronics Engineering, School of Mechanical Engineering, Pusan National University, Busan 46241, South Korea (e-mail: kshong@pusan.ac.kr).

Color versions of one or more of the figures in this paper are available online at <http://ieeexplore.ieee.org>.

Digital Object Identifier 10.1109/TCST.2017.2692745

In the last decade, comprehensive studies on the actuator saturation have led to the development of new compensation techniques for the saturation nonlinearity, addressing different aspects of the antiwindup design problems like stability, robustness, and enlargement of region of stability [5]–[9]. A linear matrix inequality (LMI)-based methodology for designing AWC using the modified sector condition is developed in [10] for linear systems in the presence of input saturation. These techniques can result in poor performance with an invalid region of stability, if employed to the nonlinear systems.

An approach has been reported in [11] for computing the static AWC gain to ensure the region of attraction of the closed-loop systems by considering an existing dynamic output feedback controller, ensuring stability of the nonlinear system in the absence of saturation. In the recent works [12], [13], AWC designs for two classes of input-constrained nonlinear systems under external disturbances and unknown direction of control gain are considered by employing the adaptive radial basis function neural networks to ensure semiglobal and global stability of the closed-loop system, respectively. AWC design for attainment of the stability, performance, and robustness under external perturbations and model uncertainties for a linear parameter varying polymer electrolyte membrane fuel cell system has been addressed in [14]. An AWC design approach for the systems containing actuator saturation and a quadratic nonlinearity has been provided in [15]. Full-order global and local decoupled-architecture-based compensation schemes were constructed for attaining stability of the nonlinear systems in [16]. M. Rehan *et al.* [17] developed the design conditions for synthesis of dynamic controller and static AWC for Lipschitz nonlinear systems under input saturation. The work of [18] demonstrated that a dynamic nonlinear internal model control-based AWC exists for a class of nonlinear systems. Further, an AWC synthesis scheme for the globally exponentially stable nonlinear systems was provided (see also [19]) to guarantee the closed-loop system's stability and \mathcal{L}_2 performance under the input saturation constraint. However, further work on the antiwindup design for the nonlinear systems is needed for addressing conservatism in the existing techniques, for AWC design of various classes of the nonlinear systems, for attainment of multiple design objectives, and for accounting experimental implementation issues.

This brief studies an antiwindup for the nonlinear parameter varying (NPV) systems under an input saturation. By employing the generalized Lipschitz continuity, quadratic Lyapunov

function, local sector condition, and \mathcal{L}_2 gain reduction for exogenous signals, an LMI-based condition for the computation of a compensator gain is explored. This brief proposes a simple static AWC design than the previously mentioned techniques and incorporates parametric variations in the nonlinear systems, which has not been reported in the previous works.

The main contribution of the proposed techniques is four-fold. First, an AWC design technique for a class of NPV systems with Lipschitz nonlinearities is addressed for the first time to the best of the author's knowledge. The proposed methodology not only allows the sector-based and Lipschitz nonlinearities but also accounts for varying parameters in a bounded range. Second, a computationally simple static AWC design technique has been explored in this brief, which is simpler than the dynamic AWC like [16] for implementation. Moreover, the observability condition for the nonlinear plant in [16] has also been relaxed in our methodology. It is notable that the proposed AWC methodology has practical significance of application to an existing control system by inducing a modest modification of the antiwindup gain and can be easily applied for attaining multiple objectives like tracking and robustness, compared with the existing approaches [17], [20]–[24]. Third, local AWC design is addressed in this brief. The local design is practicable when global stability is infeasible or performance objectives are not attainable. Last, simulation as well as experimental results of the proposed AWC approach for control of an electromechanical plant are detailed to provide both design and implementation guidelines to the readers.

The proposed antiwindup design has been validated through simulation and experimental implementation results for the speed control of a dc servo system. A dynamic feedback controller is designed using the MATLAB Simulink Response Optimization toolbox to attain the desired closed-loop system's stability and tracking performance. Further, the calibration of tachogenerator, design of a low-pass filter for noise removal, input amplification for the drive circuitry, and data acquisition are performed for interfacing the dc motor system with a computer. Nonlinearities due to armature reactance and input saturation and parametric variations due to load fluctuations are incorporated for the antiwindup design. The recent works [25]–[30] focused on the minimization of an integral square error cost function, incorporation of a reduced order observer, and utilization of a predefined PI controller to enhance the robust performance for the speed control of electric motors. In contrast, this brief addresses control of a dc motor under parametric variations and input and state nonlinearities. To the best of the authors' knowledge, static AWC design and implementation by considering the speed control problem of a nonlinear dc servo system under load variations, input saturation, and armature reactance nonlinearity has been studied for the first time. Simulation and experimental results are provided herein to demonstrate recovery from the windup condition either due to a large reference signal or because of the load variations.

Notations: Standard notations are used throughout this brief. $\bar{u} > 0$ represents the saturation bound on the control input u .

$A_{(i)}$ denotes the i th row of a matrix A . The Euclidean norm of a vector x is represented by $\|x\|$. For a vector x , $\|x\|_2 = (\int_0^\infty \|x\|^2 dt)^{1/2}$ corresponds to the \mathcal{L}_2 norm. $\text{diag}(\dots)$ represents a block diagonal matrix whose arguments are the diagonal blocks.

II. PROPOSED METHODOLOGY

Consider a class of time-varying nonlinear systems described by

$$\begin{aligned}\dot{x} &= A(\vartheta(t))x + B(\vartheta(t))u_{\text{sat}} + B_w(\vartheta(t))w + \phi(t, x, \vartheta(t)) \\ z &= C_z(\vartheta(t))x + D_z(\vartheta(t))w \\ y &= C_y(\vartheta(t))x + D_y(\vartheta(t))w\end{aligned}\quad (1)$$

where $x \in \mathbb{R}^n$ denotes the state vector, $u_{\text{sat}} \in \mathbb{R}^m$ is the standard saturated input, $w \in \mathbb{R}^p$ stands for the exogenous input (which may include one or more reference signal, disturbances, and noise), $z \in \mathbb{R}^k$ represents the exogenous output, $\phi(t, x, \vartheta(t)) \in \mathbb{R}^n$ is nonlinearity containing time-varying parameter $\vartheta(t)$, and $y \in \mathbb{R}^q$ is the measured output used for providing a feedback to controller. Each component of saturated control input is defined as $u_{\text{sat}(i)} = \text{sign}(u_{(i)})\min(\bar{u}_{(i)}, |u_{(i)}|)$, where $u_{(i)}$ is the i th component of control input. $A(\vartheta(t))$, $B(\vartheta(t))$, $B_w(\vartheta(t))$, $C_z(\vartheta(t))$, $D_z(\vartheta(t))$, $C_y(\vartheta(t))$, and $D_y(\vartheta(t))$ are linear parameter varying matrices of appropriate dimensions, containing parameter $\vartheta \in \mathbb{R}^s$ satisfying

$$Z_\vartheta = \{\theta \in \mathbb{R}^s; \theta_h \in [\underline{\vartheta}_{(h)}, \bar{\vartheta}_{(h)}]\} \quad \forall h = 1, \dots, s \quad (2)$$

where $\underline{\vartheta}_{(h)}$ and $\bar{\vartheta}_{(h)}$ are the lower and the upper bounds of time-varying parameter $\vartheta_{(h)}$. It should be clarified that $\vartheta(t)$ is a time-varying parameter of plant (1) and a parameter vector θ belongs to a convex set Z for which the parameter set is given in (2), including all possible values of the parameter $\vartheta(t)$.

Assumption 1: The nonlinearity $\phi(t, x, \vartheta)$ can be further written as $\phi(t, x, \theta) = H(\theta)f(t, x)$, where $H(\theta) \in \mathbb{R}^{n \times n}$ is a linear parameter varying matrix and the nonlinearity $f(t, x) \in \mathbb{R}^n$ for all $x, \bar{x} \in \Lambda \subseteq \mathbb{R}^n$ satisfies the conditions $\|f(t, x) - f(t, \bar{x})\| \leq \|L(x - \bar{x})\|$ and $f(t, 0) = 0, \forall t \geq 0$, where L is a matrix of appropriate dimension.

Consequently, the nonlinear system (1) can be rewritten in a more extrapolated NPV form as

$$\begin{aligned}\dot{x} &= A(\theta)x + B(\theta)u_{\text{sat}} + B_w(\theta)w + H(\theta)f(t, x) \\ z &= C_z(\theta)x + D_z(\theta)w \\ y &= C_y(\theta)x + D_y(\theta)w \quad \forall \theta \in Z.\end{aligned}\quad (3)$$

Remark 1: Clearly, the plant in (1) with time-varying parameter ϑ , satisfying the bound in (2), and containing the nonlinearity $\phi(t, x, \vartheta(t))$ validating Assumption 1, is a NPV system as seen in (3). Also note that Assumption 1 is more general than the conventional Lipschitz condition due to the consideration of L as a matrix.

For the nonlinear system (1), a given feedback controller along with AWC is represented as

$$\begin{aligned}\dot{x}_c &= A_c x_c + B_c y + E_c (u_{\text{sat}} - u) \\ u &= C_c x_c + D_c y\end{aligned}\quad (4)$$

where $x_c \in \mathbb{R}^c$ denotes the state of controller, A_c , B_c , C_c , and D_c are constant and known matrices of appropriate dimensions and E_c is the antiwindup gain. The overall closed-loop system of (3) and (4) has the form

$$\begin{aligned} \dot{\xi} &= \mathbb{A}(\theta)\xi + \mathbb{T}(\theta)w - (\mathbb{B}(\theta) + \mathbb{R}E_c)\Psi + \mathbb{F}(\theta)f(x) \\ z &= \mathbb{J}(\theta)\xi + D_z(\theta)w \\ u &= \mathbb{K}(\theta)\xi + D_c D_y(\theta)w, \quad \forall \theta \in Z \\ \xi &= \begin{bmatrix} x \\ x_c \end{bmatrix}, \quad \mathbb{A}(\theta) = \begin{bmatrix} A(\theta) + B(\theta)D_c C_y(\theta) & B(\theta)C_c \\ B_c C_y(\theta) & A_c \end{bmatrix} \\ \mathbb{B}(\theta) &= \begin{bmatrix} B(\theta) \\ 0 \end{bmatrix}, \quad \mathbb{T}(\theta) = \begin{bmatrix} B_w(\theta) + B(\theta)D_c D_y(\theta) \\ B_c D_y(\theta) \end{bmatrix} \\ \mathbb{R} &= \begin{bmatrix} 0 \\ I_{c \times c} \end{bmatrix}, \quad \mathbb{F}(\theta) = \begin{bmatrix} H(\theta) \\ 0 \end{bmatrix} \\ \mathbb{K}(\theta) &= [D_c C_y(\theta) \quad C_c], \quad \mathbb{J}(\theta) = [C_z(\theta) \quad 0], \quad \Psi = u - u_{\text{sat}}. \end{aligned} \quad (5)$$

Let us define

$$S \triangleq \{v \in \mathbb{R}^m; |u_{(i)} - v_{(i)}| \leq \bar{u}_{(i)}\}. \quad (6)$$

If the region (6) holds, the following local sector condition (see details in [2] and [31]) is satisfied:

$$\Psi^T W(v - \Psi) \geq 0. \quad (7)$$

Now a method is proposed for computation of static AWC gain E_c so that the the closed-loop system (5) in the presence of saturation nonlinearity is \mathcal{L}_2 stable.

Theorem 1: Consider the plant (1) and a controller of the form (4) such that Assumption 1 is satisfied. Suppose there exist a symmetric matrix $Q > 0$, a diagonal matrix $U > 0$, matrices V and $\mathbb{H}(\theta)$ of appropriate dimensions, and scalars κ and μ such that the set of LMIs given by

$$\begin{aligned} \kappa > 0, \quad 0 < \mu < 1 \\ \begin{bmatrix} Q & \mathbb{M}_{(i)}^T(\theta) - \mathbb{H}_{(i)}^T(\theta) \\ \star & \mu \bar{u}^2 \end{bmatrix} &\geq 0 \quad \forall \theta \in Z \\ \begin{bmatrix} \Gamma_1(\theta) & \Gamma_2(\theta) & \Gamma_3(\theta) & \mathbb{F}(\theta) & 0 & QL^T & QJ^T \\ \star & -\kappa I & D_y^T(\theta)D_c^T & 0 & D_z^T(\theta) & 0 & 0 \\ \star & \star & -2U & 0 & 0 & 0 & 0 \\ \star & \star & \star & -I & 0 & 0 & 0 \\ \star & \star & \star & \star & -I & 0 & 0 \\ \star & \star & \star & \star & \star & -I & 0 \\ \star & \star & \star & \star & \star & \star & -I \end{bmatrix} &< 0 \quad \forall \theta \in Z \end{aligned} \quad (8)$$

$$\begin{aligned} \Gamma_1(\theta) &= Q\mathbb{A}^T(\theta) + \mathbb{A}(\theta)Q \\ \Gamma_2(\theta) &= \mathbb{T}(\theta) + QJ^T(\theta)D_z(\theta) \\ \Gamma_3(\theta) &= \mathbb{H}^T(\theta) - \mathbb{B}(\theta)U - \mathbb{R}V \\ \mathbb{M}_{(i)}(\theta) &= \mathbb{K}_{(i)}(\theta)Q. \end{aligned} \quad (10)$$

are satisfied, then

- 1) the closed-loop system is locally asymptotically stable for all initial conditions $\xi^T(0)P\xi(0) \leq 1$, if $w = 0$;
- 2) the \mathcal{L}_2 gain from w to z is bounded by γ , if $w \in \mathcal{L}_2$ for all signals validating $\|w\|_2^2 \leq \delta^{-1}$;
- 3) the state of the closed-loop system remains bounded in $\xi^T(t)\mu P\xi(t) \leq 1$ for all signals satisfying $\|w\|_2^2 \leq \delta^{-1}$.

The AWC gain matrix can be calculated as $E_c = VU^{-1}$. The \mathcal{L}_2 gain bound is given by $\gamma = \sqrt{\kappa}$.

Proof: Consider a quadratic Lyapunov function

$$V(t, \xi) = \xi^T P \xi, \quad P > 0 \quad (11)$$

and define the inequality

$$J_{z1} = \dot{V}(t, \xi) + z^T z - \gamma^2 w^T w < 0. \quad (12)$$

Integrating (12) from 0 to $T \rightarrow \infty$, we have

$$\begin{aligned} \int_0^T J_{z1} dt &= (V(T, \xi) - V(0, \xi)) + \int_0^T z^T z dt \\ &\quad - \gamma^2 \int_0^T w^T w dt < 0 \end{aligned} \quad (13)$$

which has the following implications.

- 1) If $w = 0$, (12) entails that $\dot{V}(t, \xi) < 0$, i.e., the closed-loop system (5) is asymptotically stable at the origin.
- 2) If $\xi(0) = 0$, then $V(0, \xi) = 0$, which along with $V(T, \xi) > 0$ and (13) implies $\|z\|_2^2 < \gamma^2 \|w\|_2^2$, that is, the \mathcal{L}_2 gain between w and z is less than γ .

By employing (5) and by selecting $v = \mathbb{G}(\theta)\xi + D_y(\theta)w$, the region (6) can be written as

$$S \triangleq \{\xi \in \mathbb{R}^{n+c}; |\mathbb{K}_{(i)}(\theta) - \mathbb{G}_{(i)}(\theta)|\xi \leq u_{0(i)}\}. \quad (14)$$

Suppose that the region (14) remains valid for all time, then the sector condition (7) holds. Using the local sector condition, applying Assumption 1 along with (12), and defining

$$\begin{aligned} J_{z2} &= \dot{V}(t, \xi) + \Psi^T W(\mathbb{G}(\theta)\xi + D_c D_y(\theta)w - \Psi) \\ &\quad + (\mathbb{G}(\theta)\xi + D_c D_y(\theta)w - \Psi)^T W \Psi + z^T z \\ &\quad - \gamma^2 w^T w - f^T(t, x)f(t, x) + \xi^T L^T L \xi < 0 \end{aligned} \quad (15)$$

we obtain $J_{z1} < 0$, if $J_{z2} < 0$. It further entails $J_{z2} = \phi^T \Omega_1 \phi < 0$, where $\phi = [\xi^T \quad w^T \quad \Psi^T \quad f^T(t, x)]^T$ and

$$\begin{aligned} \Omega_1 &= \begin{bmatrix} \Gamma_4(\theta) & \Gamma_5(\theta) & \Gamma_6(\theta) & P\mathbb{F}(\theta) \\ \star & -\gamma^2 I + D_z^T(\theta)D_z(\theta) & D_y^T(\theta)D_c^T W & 0 \\ \star & \star & -2W & 0 \\ \star & \star & \star & -I \end{bmatrix} \\ &< 0 \quad \forall \theta \in Z \end{aligned} \quad (16)$$

$$\Gamma_4(\theta) = P\mathbb{A}(\theta) + \mathbb{A}^T(\theta)P + L^T L + J^T(\theta)J(\theta)$$

$$\Gamma_5(\theta) = P\mathbb{T}(\theta) + J^T(\theta)D_z(\theta)$$

$$\Gamma_6(\theta) = \mathbb{G}^T(\theta)W - P(\mathbb{B}(\theta) + \mathbb{R}E_c).$$

By applying the Schur complement and congruence transformation using $\text{diag}(P^{-1}, I, W^{-1}, I)$ to (16) and by selecting $Q = P^{-1}$, $U = W^{-1}$, and $\kappa = \gamma^2$, (10) is obtained. The set of LMIs in (10) ensures $J_{z2} < 0$ and resultantly $J_{z1} < 0$. Incorporating (13) and considering $(1/\gamma) \int z^T z > 0$, $\|w\|_2^2 \leq \delta^{-1}$, and $V(0, \xi) \leq 1$, we have

$$\xi(t)^T P \xi(t) \leq 1 + \gamma \delta^{-1} \quad (17)$$

which produces $\mu \xi^T(t)P\xi(t) < 1$ by application of $1 + \gamma \delta^{-1} = \mu^{-1}$ and the tolerable exogenous input bound is δ . Consequently, the region of stability $\mu \xi^T P \xi \leq 1$ holds for all time. Under $w = 0$, (12) guarantees the local asymptotic stability of the closed-loop system (5) to the origin for all initial conditions $\xi^T(0)P\xi(0) \leq 1$. Moreover, $V(T, \xi) > 0$

and (13) entail the \mathcal{L}_2 gain between w and z bounded by γ for all exogenous inputs validating $\|w\|_2^2 \leq \delta^{-1}$. The inequalities $\mu < 1$ and $\mu > 0$ are obtained as $1 + \gamma\delta^{-1} > 1$ and $1 + \gamma\delta^{-1} < \infty$, respectively.

The region (14) can be validated by including $\mu\zeta(t)^T Q^{-1}\zeta(t) \leq 1$ into (14) through

$$\zeta^T (\mathbb{K}_{(i)}^T(\theta) - \mathbb{G}_{(i)}^T(\theta))(\mathbb{K}_{(i)}(\theta) - \mathbb{G}_{(i)}(\theta))\zeta \leq \bar{u}_{(i)}^2 \quad (18)$$

which implicates (9) thereby substituting $\mathbb{H}_{(i)}(\theta) = \mathbb{G}_{(i)}(\theta)Q$ which completes the proof. \square

Remark 2: Theorem 1 addresses a fundamental static AWC design problem for the NPV systems by ensuring the local asymptotic stability and \mathcal{L}_2 stability of the closed-loop system (5). Note that novel results on static AWC design of NPV systems for global stability (under the assumption that the plant is asymptotically stable) and for zero exogenous input can be derived from Theorem 1 as specific cases by selecting $v = u$ and $w = 0$, respectively. Several static as well as dynamic AWC design conditions for different forms of the nonlinear systems have been derived in the existing works [11]–[17]. However, the work on AWC design for the NPV systems, as regarded in the present design condition, has not been addressed in the previous studies. Note that a large number of NPV systems can be found in the nature because almost all systems are nonlinear and parametric variations occur whenever a plant is operated in a wide range of conditions, like temperature, pressure, and friction.

Remark 3: In the recent studies like [16]–[19], the existence of dynamic (full-order) AWC and its design conditions for different forms of the nonlinear systems were considered. From stability and performance point of view, these AWC schemes are interesting because a dynamic compensator can be employed to attain various stability and performance objectives and its existence can be straightforward at least for the stable plants. However, implementation of such schemes may not be practical compared to the present approach due to the requirement of additional hardware/software resources and the need of rigorous implementation efforts from the practitioners.

Remark 4: A constant term Δ can be used to transform the saturation nonlinearity into the symmetric form for an unsymmetric saturation. The plant state equation in (1) and controller output equation in (4) can be rewritten as $\dot{x} = A(\vartheta(t))x + B(\vartheta(t))(u_{\text{sat}} + \Delta) + B_w(\vartheta(t))w + \phi(t, x, \vartheta(t))$ and $u = C_c x_c + D_c y - \Delta$, respectively. Note that these additions do not alter the overall closed-loop system (5); therefore, the proposed AWC design approaches can be straightforwardly employed for the computation of AWC gain.

We develop an algorithm for solving the set of LMIs of Theorem 1 by considering a 2-D gridding of the parameter set in order to obtain the antiwindup gain E_c . Let the variation in each parameter be defined as $\theta_1 \in [\theta_{11}, \theta_{1q}]$, $\theta_2 \in [\theta_{21}, \theta_{2q}], \dots, \theta_r \in [\theta_{r1}, \theta_{rq}]$, where $\theta_{i1} = \underline{\vartheta}_{(i)}$ and $\theta_{iq} = \bar{\vartheta}_{(i)}$. Consider the step size for each parameter as $(\epsilon_1, \epsilon_2, \dots, \epsilon_s)$, where $\epsilon_i = (\theta_{iq} - \theta_{i1})/q$ and q^s denotes the total number of points employed in the algorithm.

Algorithm 1: The set of LMIs in Theorem 1 are solved in the following steps:

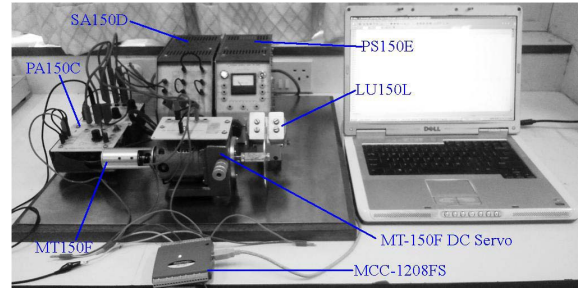


Fig. 1. MS-150 system interfaced with computer through MCC-1208FS.

- 1) Initialize $i = 1, j = 1$.
- 2) Construct the LMIs of Theorem 1 by assigning $\theta = \theta_{ij}$.
- 3) Increment j . If $j \leq q$, compute $\theta_{ij} = \theta_{i(j-1)} + \epsilon_i$ and goto Step 2, otherwise set $j = 1$.
- 4) Increment i . If $i \leq s$, goto Step 2.
- 5) Solve the set of LMIs obtained in Step 2 for the variables $Q, U, V, \mathbb{H}(\theta), \kappa$ and μ .
- 6) Compute E_c by solving $E_c = VU^{-1}$.

III. SIMULATION AND EXPERIMENTAL IMPLEMENTATION

For analysis and testing of the proposed antiwindup scheme, a benchmark system MS-150 manufactured by Feedback Instrumentation Ltd. has been employed. It consists of a power supply unit (PS150E), servo amplifier unit (SA150D), pre-amplifier unit (PA150C), dc servo motor and tachogenerator component (MT150F), and braking unit (LU150L). The experimental setup with labels of different components is shown in Fig. 1. For data acquisition, MCC-1208FS card has been interfaced with MS-150 to control the motor speed through a computer.

A. Nonlinear Motor Model

The nonlinear motor model (see [32]) with saturated control input (u_{sat}) has the form

$$\begin{aligned} \dot{\omega} &= -\frac{F}{J}\omega + \frac{a}{J}i + \frac{b}{J}i^2 - \frac{1}{J}T_l \\ \dot{i} &= -\frac{a}{L}\omega - \frac{b}{L}\omega i - \frac{R}{L}i + \frac{\lambda}{L}u_{\text{sat}} \end{aligned} \quad (19)$$

where $L, i, a, b, R, \lambda, J, \omega, F$, and T_l are the armature inductance, armature current, no load machine constant, a small negative number, armature resistance, circuitry gain, motor inertia, rotor rotation speed, motor viscous friction constant, and torque applied to the rotor by an external load, respectively. The angular speed of the motor measured in revolution per minute (rpm) is defined as y_s and given by $y_s = (60/(2\pi))\omega$. Then the error and the exogenous output signals are selected as $z = e = r - y_s$, where r is the reference input (rpm).

B. AWC and Controller Design

The nonlinear motor parameters are given in Table I. The motor inertia has variation in the range defined by $J \in [0.012, 0.055]$. Let us assign $[x_1 \ x_2]^T = [\omega \ i]^T$. By using

TABLE I
PARAMETERS OF THE NONLINEAR DC SERVO MOTOR SYSTEM

Parameter	Value	Parameter	Value
$R(\Omega)$	3.2	$F(\text{Nm s/rad})$	0.01
$a(\text{V/rad})$	60×10^{-3}	$b(\Omega/\text{rad})$	-0.01
$L(\text{H})$	8.6×10^{-3}	Ampifier Current Limit	2 A
Gear ratio	30:1	λ	17.5

the values of the parameters given in Table I, the nonlinear dc motor model (19) can be transformed into (1) by using $\vartheta(t) = J^{-1}$, where the region (2) is defined as

$$Z_v = \{\theta \in \mathbb{R}; \theta \in [18.18, 83.33]\}. \quad (20)$$

The system matrices are given by

$$A(\theta) = \begin{bmatrix} -0.01\theta & 0.006\theta \\ -6.9767 & -372.093 \end{bmatrix}, \quad B(\theta) = \begin{bmatrix} 0 \\ 6104.65 \end{bmatrix}$$

$$B_w(\theta) = \begin{bmatrix} 0 & -\theta \\ 0 & 0 \end{bmatrix}, \quad f(t, \omega, i) = \begin{bmatrix} -0.01\theta i^2 \\ 1.666\omega i \end{bmatrix}$$

$$C_z(\theta) = C_y(\theta) = [-9.54929 \ 0], \quad D_z(\theta) = D_y(\theta) = [1 \ 0].$$

The dc motor model considered herein consists of two state variables; however, the nonlinear terms, input saturation, and parametric variations establish the overall motor system as a highly nonlinear plant. The nonlinearity in the dc motor system, usually ignored under low speed and low load assumptions, causes adverse effects under the large load variations and high speed operating conditions. It should also be noted that the scope of the proposed AWC design approach is not limited, as these AWC schemes can also be applied to other complicated nonlinear systems. A PI controller is designed using MATLAB Simulink Response Optimization toolbox for 15% overshoot, 6 s settling time, and 1.5 s rise time for the nonlinear plant (19) by neglecting the input saturation. The controller is given by

$$\dot{x}_c = y \quad u = 0.0009 \times 3x_c + 0.002 \times 3y. \quad (21)$$

The data acquisition card (DAC) MCC-1208FS has an output voltage limit of $0 - 4$ V and the saturation bound for control signal of the preamplifier unit is 12 V. To address the limitation of the DAC, we convert the controller (21) into two cascaded controllers (i.e., one PI controller and the other proportional gain and controller bias). The cascade form of the controller is given by

$$\dot{x}_c = y$$

$$\tilde{u} = 0.0009x_c + 0.002y - \Delta \quad (22)$$

$$u_{\text{sat}} = 3(\tilde{u}_{\text{sat}} + \Delta). \quad (23)$$

As $\tilde{u} = u - \Delta$, the saturation limit of \tilde{u} becomes ± 2 V for $\Delta = 2$ V. To compute the AWC gain E_c , the LMIs (9) and (10) in Theorem 1 are solved by using multiple points including vertices of (20). Various matrices and parameters are

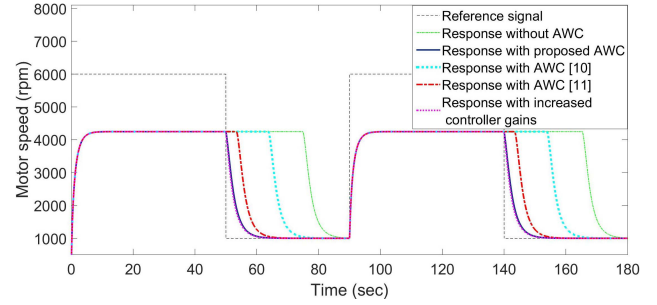


Fig. 2. Closed-loop responses for testing the proposed method.

computed as

$$Q = \begin{bmatrix} 2.8908 \times 10^5 & -5.5460 \times 10^4 & 3.0461 \times 10^6 \\ -5.5460 \times 10^4 & 1.6406 \times 10^7 & 6.4649 \times 10^5 \\ 3.0461 \times 10^6 & 6.4649 \times 10^5 & 6.3829 \times 10^7 \end{bmatrix}$$

$$H = [-311.6148 \quad -1.7661 \times 10^3 \quad -2.4582 \times 10^4]^T$$

$$\mu = 0.738, \quad E_c = 99.989, \quad U = 122.662, \quad \gamma = 2.91 \times 10^4.$$

Therefore, the first stage of controller containing the static AWC has the form

$$\dot{x}_c = y + 99.9896 \times 3(\tilde{u}_{\text{sat}} - \tilde{u})$$

$$\tilde{u} = 0.0009x_c + 0.002y - \Delta \quad (24)$$

where the factor of 3 is used because $u_{\text{sat}} - u = 3(\tilde{u}_{\text{sat}} - \tilde{u})$. Before moving toward the experimental implementation results, we test our AWC design approach by comparing with the existing works and by accounting for the uncertainty and the change in controller parameters. The AWC gains obtained by the methodologies [11] and [10] are 31.98 and 6.40, respectively, for the nominal selection of $J = 0.012$. Fig. 2 provides several closed-loop responses by applying the proposed AWC and the existing methods. To account for the uncertainty, we have changed the value of inertial load to $J = 0.0492$. It can be observed from the plots that the response of the proposed AWC is tracking the reference signal without a lag. While the approaches in [10] and [11] are not completely compensating the windup effects due to the lags caused by the input saturation. In another experiment, we increased the controller parameters C_c and D_c to 10% to study the effect of variation in control parameters. The response due to variation of the controller parameters with the proposed AWC is closer to the response without accounting the change in parameters. Hence, the proposed AWC methodology has a better response compared with the existing approaches due to consideration of the nonlinear and parametric variations. In addition, the response of the proposed AWC is robust against the load and controller parameter variations.

C. Experimental Implementation

The proposed AWC and cascade controllers are implemented for computer-based control of the MS-150 dc servo system. The block diagram of the overall closed-loop system with the proposed AWC, controller, and various interfacing and signal processing blocks is shown in Fig. 3.

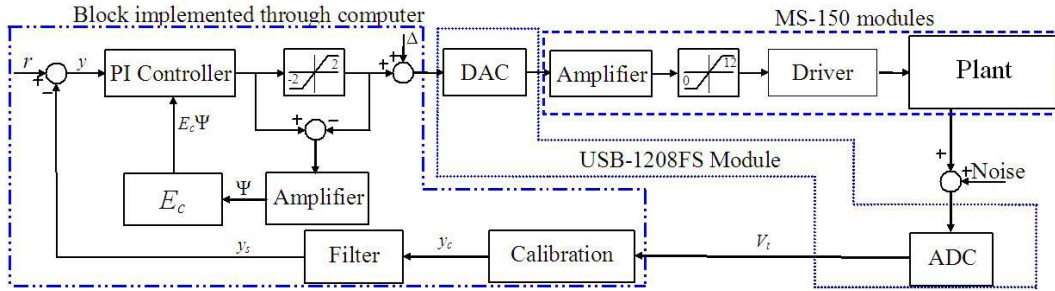


Fig. 3. Block diagram demonstrating implementation of the proposed AWC and controller for the NPV servo system.

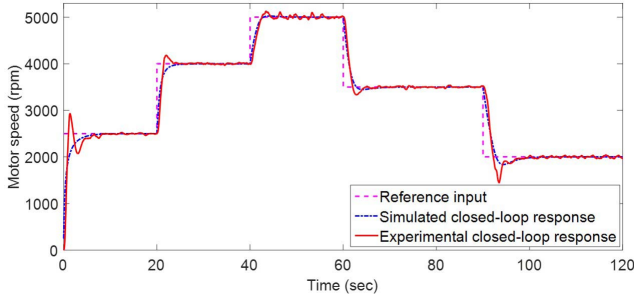


Fig. 4. Closed-loop response of the system under stair-case reference.

The tachogenerator output denoted by V_t is taken into computer through MCC-1208FS interfacing card and the angular speed of the motor is calculated using the tachogenerator voltage V_t through a calibration equation. The calibrated output, subjected to the measurement noise, is represented as y_c . A six-order polynomial is employed for the calibration purpose, which is given by

$$y_c = 856V_t^6 - 5735V_t^5 + 1.453 \times 10^4 V_t^4 - 1.75 \times 10^4 V_t^3 + 1.033 \times 10^4 V_t^2 - 315.5 V_t + 255.4.$$

Since the output y_c contains measurement noise, a second order low-pass filter is applied to obtain the measured angular speed of the motor. By considering the filter quality factor of 0.5 and 3 dB bandwidth 1.4468, the transfer function of the filter is given as

$$F(s) = \frac{1}{0.0484s^2 + 0.44s + 1}. \quad (25)$$

Discretization of the low-pass filter using bilinear approximation for a sampling time of 0.02 s is accomplished and the filter is implemented through a computer. The second stage of controller (23) is implemented via the amplifier block SA150D with a gain of three. The PI controller (24) is discretized using bilinear approximation with a sampling time of 0.02 s. The PI control stage and AWC (24) are implemented via a computer program.

D. Simulation and Experimental Results

The nonlinear model is simulated in MATLAB using S-function blocks of Simulink, which allow simulation of user-defined dynamic models. The closed-loop system is formed by considering the nonlinear plant (19) and cascade controllers (22) and (23). In order to check the tracking

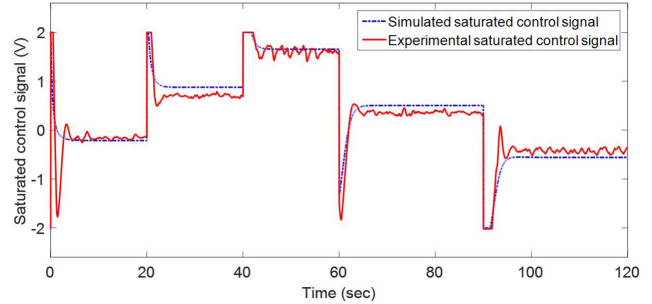


Fig. 5. Saturated control signal under stair-case reference.

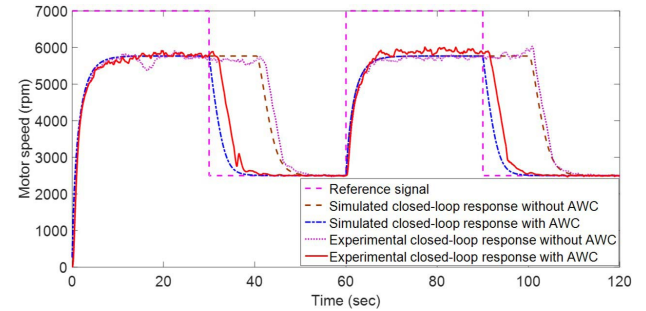


Fig. 6. Closed-loop response of the system under square-wave reference.

performance of the proposed control strategy of Fig. 3, a stair-case reference signal as shown in Fig. 4 is applied in the absence of an AWC and no load variation. It is observed that the associated output of the closed-loop system is faithfully following the reference with the desired specifications in both simulation and experimental results. Fig. 5 shows the simulated and experimental saturated control signal \tilde{u} of the first stage (22). Despite that the control signal of Fig. 5 is saturated, the closed-loop response is not affected by the windup consequences. The experimental saturated control signal and the associated output show similar results as obtained during the simulation. The effect of saturation nonlinearity is not enough to produce lag due to windup effect as neither the large reference signal nor the loading effects are considered in Figs. 4 and 5.

In order to analyze the windup effects, the reference signal as shown in Fig. 6 is applied without considering the effects of load variations. Like disturbances and perturbations, reference signals with large amplitudes can result into accumulation of the error at the control signal. Therefore, it is viable to apply such a reference signal to test the windup effect and antiwindup performance. Since the control signal is saturated

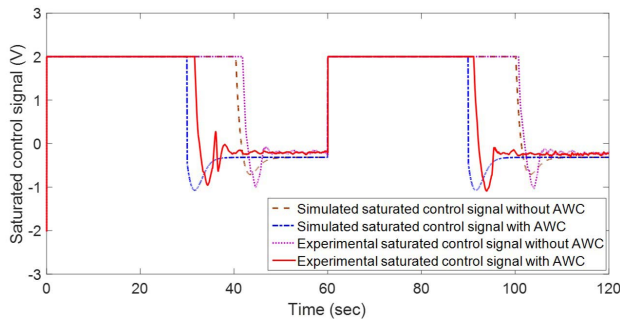


Fig. 7. Saturated control signal under square-wave reference.

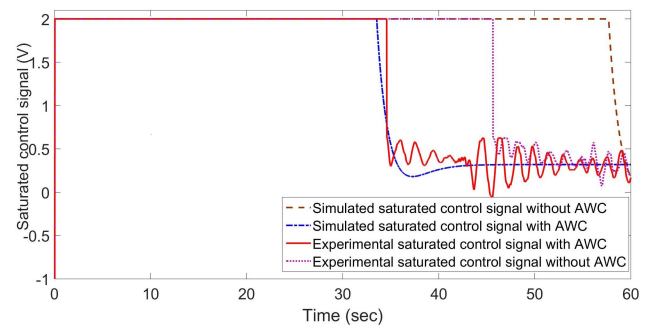


Fig. 9. Saturated control signal under load variations.

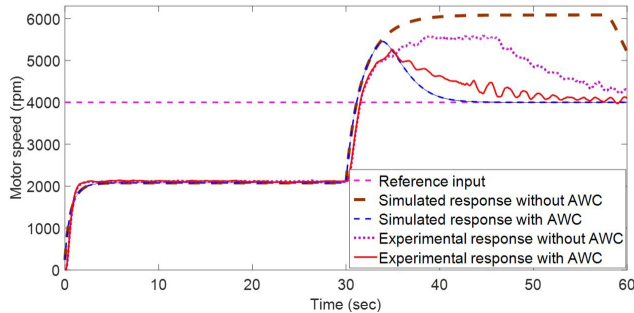


Fig. 8. Closed-loop response of the system under load variations.

due to large amplitude of the reference signal, the windup effect is clearly observed in the motor speed response of Fig. 6 and the controller (22) output of Fig. 7. The motor speed response has a lag due to the saturation of the control signal. The proposed AWC is applied in order to remove the windup effects. Clearly, the motor angular speed lag in following the reference input has been removed by the application of the proposed static AWC. Hence, the performance degradation caused by the windup effects can be addressed by using the proposed compensator. It should also be noted that the experimental results are closer to the simulation results detailed in Figs. 6 and 7.

In another experiment, we observe the effects of windup and improvement of the response through the proposed AWC by considering the loading effects on the servo motor system. The load variations are considered by first adding the load for 30 s and then removing the load on the motor shaft such that the motor inertia is varied in the range given as $J \in [0.012, 0.055]$. On the experimental setup, the magnetic loading effects are tested using the loading unit LU150L in order to study the closed-loop system performance. The loading unit is positioned at the brake at a scale of 5 in the start and then changed to 0 scale at a time of 30 s. Fig. 8 shows the simulation and experimental results of the motor output response in the presence of load variations for the two cases of absence of an AWC and incorporation of the proposed AWC. Throughout this experiment, the reference signal is kept constant. When the load is removed, the output response without any AWC shows a lag in tracking the reference signal, while the output response due to the proposed AWC immediately follows the reference signal. The corresponding simulation and experimental results of control signals without an AWC and with the proposed AWC are demonstrated in Fig. 9.

It should also be noted that the experimental results have some variations with the simulation study of Figs. 8 and 9; although the same conclusion of improvement of the response using the proposed AWC can be drawn from both cases. The simulation results demonstrate that the motor control signal remains saturated for a longer interval than the experimental results for the no AWC case. Since the loading unit applies magnetic properties, which may have been deteriorated with time, causing a less degree of windup effects. The windup effects can be removed by employing the proposed AWC and the output settles at the set point, improving the system performance as seen in the experimental results, similar to the simulations. Hence, the proposed AWC methodology can be employed to overcome the accumulation of the integral effects of input saturation in controlling the speed of a NPV dc motor.

Remark 5: This section provided an antiwindup-based control study of a dc servo system in the presence of input saturation, armature nonlinearity, and load variations. A detailed guideline for the design and implementation of a static antiwindup and controller by transforming the nonlinear servo system with parametric changes into an NPV system has been provided. Various simulation and experimental studies like [25]–[30] have been focused in the literature on angular speed control of the servo systems. Unlike these studies, the present approach focused a nonlinear servo system model with parametric variations and input saturation; and both simulation and experimental results are provided along with the implementation details. To the best of the authors' knowledge, an experimental study for the control of a dc servo system, based on static AWC, by taking a complex scenario of actuator saturation, armature nonlinearity, and load variations into account has been addressed for the first time. From the industrial application point of view, these results are promising because of a large number of applications of the servo systems and frequent appearance of nonlinearities and load changes, causing performance degradation of electromechanical motors.

The present servo control application considered modification of PI controller for an AWC to improve performance in the presence of saturation. Note that the proposed approach in Theorem 1 cannot be applied to design AWC for nonlinear controller. Further studies can be taken into account for advanced adaptive fuzzy, fuzzy PID, and neuro fuzzy controller [33]–[35] to incorporate AWC for attaining remarkable closed-loop performance. These approaches provide a better closed-loop performance for the linear region of the

control signal. However, the performance is restricted when the control signal saturates; therefore, windup compensation can be investigated to improve the nonlinear control signal performance.

IV. CONCLUSION

This brief studied the AWC design for the NPV systems with input saturation. The condition for designing static AWC, ensuring local stability of the closed-loop system, was formulated by employing the stability theories and sector condition. Compared with the previous works on nonlinear systems, the present design approach is useful for dealing with the parametric variations, for straightforward control system design, to obtain computationally simple AWC, to assure uncomplicated implementation, and for modifying existing control architectures. The proposed AWC approach was applied to control a nonlinear dc servo system, both simulation and experimental results having similar performance, were demonstrated. Nonlinearities due to the input saturation and armature current and, further, parametric variations of the motor inertia were incorporated for the control system synthesis. Various steps like modeling, controller design, AWC design, design verification, interfacing, calibration, filtering, and implementation of the controller and AWC were detailed. The proposed AWC methodology was tested for a square-wave reference signal with large amplitude and for load variations. The resultant approach is found to be effective in improving the closed-loop system response and control signal against the windup consequences.

REFERENCES

- [1] S. Galeani, S. Tarbouriech, M. Turner, and L. Zaccarian, "A tutorial on modern anti-windup design," *Eur. J. Control*, vol. 15, nos. 3–4, pp. 418–440, 2009.
- [2] S. Tarbouriech and M. Turner, "Anti-windup design: An overview of some recent advances and open problems," *IET Control Theory Appl.*, vol. 3, no. 1, pp. 1–19, 2009.
- [3] S. Tarbouriech, G. Garcia, J. M. Gomes da Silva, Jr., and I. Queinnec, *Stability and Stabilization of Linear Systems With Saturating Actuators*. London, U.K.: Springer, 2011.
- [4] L. Zaccarian and A. R. Teel, *Modern Anti-Windup Synthesis: Control Augmentation for Actuator Saturation*. Princeton, NJ, USA: Princeton Univ. Press, 2011.
- [5] A. Saberi, Z. Lin, and A. R. Teel, "Control of linear systems with saturating actuators," *IEEE Trans. Autom. Control*, vol. 41, no. 3, pp. 368–378, Mar. 1996.
- [6] M. C. Turner, G. Herrmann, and I. Postlethwaite, "Incorporating robustness requirements into antiwindup design," *IEEE Trans. Autom. Control*, vol. 52, no. 10, pp. 1842–1855, Oct. 2007.
- [7] Y. Li and Z. Lin, "Design of saturation-based switching anti-windup gains for the enlargement of the domain of attraction," *IEEE Trans. Autom. Control*, vol. 58, no. 7, pp. 1810–1816, Jul. 2013.
- [8] K. Sawada, T. Kiyama, and T. Iwasaki, "Generalized sector synthesis of output feedback control with anti-windup structure," *Syst. Control Lett.*, vol. 58, no. 6, pp. 421–428, 2009.
- [9] G. Grimm, J. Hatfield, I. Postlethwaite, A. R. Teel, M. C. Turner, and L. Zaccarian, "Antiwindup for stable linear systems with input saturation: An LMI-based synthesis," *IEEE Trans. Autom. Control*, vol. 48, no. 9, pp. 1509–1525, Sep. 2003.
- [10] J. M. G. D. Silva and S. Tarbouriech, "Antiwindup design with guaranteed regions of stability: An LMI-based approach," *IEEE Trans. Autom. Control*, vol. 50, no. 1, pp. 106–111, Jan. 2005.
- [11] J. M. Gomes da Silva, Jr., M. Z. Oliveira, D. Coutinho, and S. Tarbouriech, "Static anti-windup design for a class of nonlinear systems," *Int. J. Robust Nonlinear Control*, vol. 24, no. 5, pp. 793–810, 2014.
- [12] J. Ma, S. S. Ge, Z. Zheng, and D. Hu, "Adaptive NN control of a class of nonlinear systems with asymmetric saturation actuators," *IEEE Trans. Neural Netw. Learn. Syst.*, vol. 26, no. 7, pp. 1532–1538, Jul. 2015.
- [13] J. Ma, Z. Zheng, and P. Li, "Adaptive dynamic surface control of a class of nonlinear systems with unknown direction control gains and input saturation," *IEEE Trans. Cybern.*, vol. 45, no. 4, pp. 728–741, Apr. 2015.
- [14] F. D. Bianchi, C. Kunusch, C. Ocampo-Martinez, and R. S. Sánchez-Peña, "A gain-scheduled LPV control for oxygen stoichiometry regulation in PEM fuel cell systems," *IEEE Trans. Control Syst. Technol.*, vol. 22, no. 5, pp. 1837–1844, Sep. 2014.
- [15] G. Valmórbida, S. Tarbouriech, M. Turner, and G. Garcia, "Anti-windup design for saturating quadratic systems," *Syst. Control Lett.*, vol. 62, no. 5, pp. 367–376, May 2013.
- [16] M. Rehan and K.-S. Hong, "Decoupled-architecture-based nonlinear anti-windup design for a class of nonlinear systems," *Nonlinear Dyn.*, vol. 73, no. 3, pp. 1955–1967, Aug. 2013.
- [17] M. Rehan, A. Q. Khan, M. Abid, N. Iqbal, and B. Hussain, "Anti-windup-based dynamic controller synthesis for nonlinear systems under input saturation," *Appl. Mathe. Comput.*, vol. 220, pp. 382–393, Sep. 2013.
- [18] G. Herrmann, P. P. Menon, M. C. Turner, D. G. Bates, and I. Postlethwaite, "Anti-windup synthesis for nonlinear dynamic inversion control schemes," *Int. J. Robust Nonlinear Control*, vol. 20, no. 13, pp. 1465–1482, 2010.
- [19] G. Herrmann, M. C. Turner, P. Menon, D. G. Bates, and I. Postlethwaite, "Anti-windup synthesis for nonlinear dynamic inversion controllers," *Proc. IFAC*, vol. 39, no. 9, pp. 471–476, 2006.
- [20] E. F. Mulder, P. Y. Tiwari, and M. V. Kothare, "Simultaneous linear and anti-windup controller synthesis using multiobjective convex optimization," *Automatica*, vol. 45, no. 3, pp. 805–811, 2009.
- [21] E. F. Mulder and M. V. Kothare, "Static anti-windup controller synthesis using simultaneous convex design," in *Proc. Amer. Control Conf.*, vol. 1, May 2002, pp. 651–656.
- [22] E. F. Mulder, M. V. Kothare, and M. Morari, "Multivariable anti-windup controller synthesis using iterative linear matrix inequalities," in *Proc. Eur. Control Conf.*, Aug. 1999, pp. 3531–3536.
- [23] N. Wang, H. Pei, and Y. Tang, "Anti-windup-based dynamic controller synthesis for Lipschitz systems under actuator saturation," *IEEE/CAA J. Auto. Sinica*, vol. 2, no. 4, pp. 358–365, Oct. 2015.
- [24] S. Formentin, F. Dabbene, R. Tempo, L. Zaccarian, and S. M. Savaresi, "Scenario optimization with certificates and applications to anti-windup design," in *Proc. IEEE Conf. Decision Control*, Dec. 2014, pp. 2810–2815.
- [25] A.-A. Ahmadi, F. R. Salmasi, M. Noori-Manzar, and T. A. Najafabadi, "Speed sensorless and sensor-fault tolerant optimal PI regulator for networked dc motor system with unknown time-delay and packet dropout," *IEEE Trans. Ind. Electron.*, vol. 61, no. 2, pp. 708–717, Feb. 2014.
- [26] Y. I. Son, I. H. Kim, D. S. Choi, and H. Shim, "Robust cascade control of electric motor drives using dual reduced-order PI observer," *IEEE Trans. Ind. Electron.*, vol. 62, no. 6, pp. 3672–3682, Jun. 2015.
- [27] H. N. Tien, C. W. Scherer, J. M. A. Scherpen, and V. Müller, "Linear parameter varying control of doubly fed induction machines," *IEEE Trans. Ind. Electron.*, vol. 63, no. 1, pp. 216–224, Jan. 2015.
- [28] J. W. Choi and S. C. Lee, "Antiwindup Strategy for PI-Type Speed Controller," *IEEE Trans. Ind. Electron.*, vol. 56, no. 6, pp. 2039–2046, Jun. 2009.
- [29] P. March and M. C. Turner, "Anti-windup compensator designs for non-salient permanent-magnet synchronous motor speed regulators," *IEEE Trans. Ind. Appl.*, vol. 45, no. 5, pp. 1598–1609, Sep./Oct. 2009.
- [30] C. L. Hoo, S. M. Harris, E. C. Y. Chung, and N. A. N. Mohamed, "New integral antiwindup scheme for PI motor speed control," *Asian J. Control*, vol. 17, no. 6, pp. 2115–2132, Nov. 2015.
- [31] S. Tarbouriech, C. Prieur, and J. M. G. D. Silva, "Stability analysis and stabilization of systems presenting nested saturations," *IEEE Trans. Autom. Control*, vol. 51, no. 8, pp. 1364–1371, Aug. 2006.
- [32] G. G. Rigatos, "Particle and Kalman filtering for state estimation and control of DC motors," *ISA Trans.*, vol. 48, no. 1, pp. 62–72, Jan. 2009.
- [33] K. Premkumar and B. V. Manikandan, "Adaptive fuzzy logic speed controller for brushless DC motor," in *Proc. Power, Energy Control*, Feb. 2013, pp. 290–295.
- [34] K. Premkumar and B. V. Manikandan, "Fuzzy PID supervised online ANFIS based speed controller for brushless DC motor," *Neurocomputing*, vol. 157, pp. 76–90, Jun. 2015.
- [35] K. Premkumar and B. V. Manikandan, "Adaptive neuro-fuzzy inference system based speed controller for brushless DC motor," *Neurocomputing*, vol. 138, pp. 260–270, Aug. 2014.